ISSN 1070-3284, Russian Journal of Coordination Chemistry, 2009, Vol. 35, No. 4, pp. 279–285. © Pleiades Publishing, Ltd., 2009.
Original Russian Text © V.V. Gorinchoi, K.I. Turte, Yu.A. Simonov, S.G. Shova, Ya. Lipkovskii, V.N. Shofranskii, 2009, published in Koordinatsionnaya Khimiya, 2009, Vol. 35, No. 4, pp. 283–290.

Heteronuclear {Fe-Ba, Fe-Sr} Salicylate Complexes. Synthesis, Structure, and Physicochemical Properties

V. V. Gorinchoi[a], K. I. Turte[a]*, Yu. A. Simonov[b], S. G. Shova[b], Ya. Lipkovskii[c], and V. N. Shofranskii[a]

[a] *Institute of Chemistry, Academy of Sciences of Moldova, Chisinau, Moldova*
[b] *Institute of Applied Physics, Academy of Sciences of Moldova, Chisinau, Moldova*
[c] *Institute of Physical Chemistry, Warsaw, Poland*
**E-mail: turtae@yahoo.com*

Received June 4, 2008

Abstract—The reactions of strontium and barium salicylates with iron nitrate gave heterometallic complexes $\{[FeSr_2(Sal)_2(SalH)_2(NO_3)(DMA)_4]\}_n$ (**I**) and $\{[FeBa_2(Sal)_2(SalH)_3(DMA)_4(H_2O)]\}_n$ (**II**). The solid compounds are one-dimensional coordination polymers where bridging function is performed by salicylic acid residues and the NO_3^- group (in **I**). The salicylic acid residues are coordinated in the chelating bridging mode, their denticity ranging from 2 to 5. The IR spectra, magnetic properties, and thermal behavior of the complexes were studied.

DOI: 10.1134/S1070328409040083

Transition metal clusters with carboxylic acids as ligands are of both theoretical and practical interest [1]. Polynuclear carboxylates containing iron atoms as cores are successfully used to model the active sites of iron proteins such as hemerythrin [2], methane monooxygenase [3, 4], ribonucleotide reductase [4], and so on. Recently iron clusters have aroused much interest as they can be used, along with manganese carboxylates, for the design of molecular magnets [5].

Currently iron clusters with mono- and dibasic carboxylic acid bridges have been studied rather comprehensively. However, only few publications are devoted to the synthesis and investigation (especially by X-ray diffraction) of heteronuclear coordination compounds of iron with hydroxycarboxylic acids, in particular, salicylic acid and its residues ($C_6H_4(OH)COOH = SalH_2$, $C_6H_4(OH)COO^- = SalH^-$, $C_6H_4(O^-)COO^- = Sal^{2-}$). Like other divalent metal ions, Fe^{2+} ions form two series of salts: $Fe(SalH)_2$ and Fe(Sal), whereas trivalent iron compounds include $Fe(SalH)_3$, Fe(SalH)(Sal), $Fe_2(Sal)_3$, etc. If other ligands are present in the solution (e.g. OH^-, H_2O), mixed-ligand complexes can be formed [6–9].

Note that coordination compounds of salicylic acid with metals have found practical use as precursors in the synthesis of new compounds, in the oxidative destruction of flammable combustible polystyrenes [7], for increasing corrosion protection of internal combustion engines [10–12], and in the search for new active biological agents [13].

This paper presents data on the synthesis and X-ray diffraction study of two polynuclear heterometallic iron complexes with barium and strontium: $\{[FeSr_2(SalH)_2(Sal)_2(NO_3)(DMA)_4]\}_n$ (**I**), and $\{[FeBa_2(Sal)_2(SalH)_3(DMA)_4(H_2O)]\}_n$ (**II**), where DMA is dimethylacetamide. Preliminary results of these studies were published previously [14–17].

EXPERIMENTAL

The starting compounds $Sr(SalH)_2 \cdot 3H_2O$ and $Ba(SalH)_2 \cdot H_2O$ were prepared by the reaction of strontium carbonate or barium hydroxide, respectively, with salicylic acid. The other reagents (CH_3OH, DMA, THF) were commercial chemicals used as received.

Synthesis of I. $Fe(NO_3)_3 \cdot 9H_2O$ (1 g, 2.47 mmol) was added with continuous stirring to $Sr(C_6H_4(OH)COO)_2 \cdot 3H_2O$ (3.76 g, 9.88 mmol) in methanol (25 ml). After 30 min, the resulting solution was filtered and evaporated to dryness on a water bath. A solvent mixture (18 ml of THF and 7 ml of DMA) was added to the dried residue. After stirring for 20 min at room temperature, the resulting dark red solution was filtered and left in air at room temperature. After 4 weeks, crystals of **I** precipitated as dark red rectangular prisms. Yield 2.56 g (86% relative to the strontium salt).

For $C_{44}H_{54}FeN_5O_{19}Sr_2$	
anal. calcd, %:	C, 44.48; H, 4.58; N, 5.89; Fe, 4.70; Sr, 14.75.
Found, %:	C, 43.88; H, 4.55; N, 5.93; Fe, 4.88; Sr,14.73.

IR (ν, cm^{-1}): 3070 m, 2990 s, 2880 sh, 1620 s, 1570 s, 1600 m, 1580 sh, 1518 m, 1470 m, 1452 s, 1423 m,

Table 1. Crystal data for complexes **I** and **II**

Parameter	Value	
	I	**II**
M	1188.01	1380.57
Space group	$P2_1/c$	$P2_1/c$
Unit cell parameters:		
a, Å	9.2180(2)	19.3711(2)
b, Å	29.9710(12)	16.8593(2)
c, Å	18.0210(6)	18.5731(2)
β, deg	92.180(2)	109.7860(10)
V, Å^3	4975.1(3)	5707.56(11)
Z	4	4
ρ(calcd), g/cm^3	1.586	1.607
μ_{Mo}, mm^{-1}	2.504	1.692
F(000)	2428	2772
Ranges of θ angles, deg	2.21–25.00	1.65–27.00
Index ranges	$-10 \le h \le 10$, $-28 \le k \le 35$, $-21 < l < 21$	$-24 \le h \le 0$, $-21 \le k \le 21$, $-22 \le l \le 23$
The number of reflections	12826	38275
The number of independent reflections, $I > 2\sigma(I)$	8630 (R_{int} = 0.0644)	12446 (R_{int} = 0.0268)
The data collection extent to θ_{max}, %	98.6	99.9
The number of refined parameters	636	793
GOOF on F^2	1.050	1.069
Final R-factors $I > 2\sigma(I)$	R_1 = 0.0848, wR_2 = 0.1578	R_1 = 0.0263, wR_2 = 0.0500
R-factors for all reflections	R_1 = 0.1390, wR_2 = 0.1785	R_1 = 0.0325, wR_2 = 0.0600
$\Delta\rho_{max}$ and $\Delta\rho_{min}$, e Å^{-3}	0.730 and –0.804	0.801 and –0.606

1375 s, 1320 m, 1305 m, 1290 m, 1180 sh, 1140 m, 1090 w, 1035 m, 1015 m.

Synthesis of II was carried out as described for **I** using $Ba(C_6H_4(OH)COO)_2 \cdot H_2O$ instead of $Sr(C_6H_4(OH)COO)_2 \cdot 3H_2O$.

The dark red single crystals as rectangular prisms precipitated after 4 weeks. Yield 0.81 g (76% relative to the barium salt).

For $C_{51}H_{61}Ba_2FeN_4O_{22}$			
anal. calcd, %:	C, 44.36;	H, 4.45;	N, 4.05.
Found, %:	C, 44.57;	H, 4.87;	N, 3.69.

IR (ν, cm^{-1}): 3434 s, 3059 w, 2942 w, 2864 sh, 1622 s, 1600 sh, 1576 sh, 1485 s, 1456 s, 1512 w, 1391 s, 1360 s, 1322 sh, 1253 s, 1218 m, 1186 s, 1143 s, 1132 w, 1100 sh, 1042 w, 1021 w, 1016 sh.

Analysis for C, H, and N of **I** and **II** was performed by the elemental analysis group of the Institute of Chemistry (Academy of Sciences of Moldova); the metals were determined at the Center of Metrology and Analytical Research Methods (Academy of Sciences of Moldova) on an AAS-1N atomic absorption spectrometer (Karl Zeiss).

X-Ray Diffraction. The experimental data for **I** and **II** were collected at 100 K on a Nonius Kappa CCD diffractometer (MoK_α radiation, λ = 0.71073 Å, graphite monochromator, ω-2θ scan mode). The unit cell parameters were refined for the whole array of experimental data. The intensity integration and reduction to a common scale were performed by DENZO and SKALEPACK software [18]. Absorption corrections were applied using XEMP software [19].

The structures of **I** and **II** were solved by the direct method and refined by the least-squares method in the anisotropic full-matrix approximation for non-hydrogen atoms (SHELX-97 [20]). The hydrogen positions in **I** were found objectively, those in **II** were calculated geometrically and refined isotropically in the rigid body model. The refinement revealed disorder of dimethylacetamide molecule and the hydoxyl oxygen in one acid residue of **II**.

The key X-ray experiment details, structure solution and refinement data for **I** and **II** are summarized in Table 1, and selected interatomic distances and bond angles are in Table 2. Atom coordinates and other structural parameters for **I** and **II** are deposited with the Cambridge Crystallographic Data Centre (no. 688416 for **I** and no. 688415 for **II**).

IR spectra were recorded on a Specord M75 spectrometer in the 400–4000 cm^{-1} range (mineral or fluorinated oil mulls).

Complex thermal analysis (CTA) was carried out on a Paulik–Paulik–Erdey derivatograph in air with Al_2O_3 as the standard. Recording conditions: DTG, 1/5; DTA, 1/10; TG, 100/100; T_{max} = 800°C; heating rate 5 K/min; 100 mg samples.

The magnetic properties of complexes **I** and **II** were studied by the Gouy method at room temperature (293 K) at a setup of the Institute of Chemistry (Academy of Sciences of Moldova). As the reference for magnetic susceptibility calibration, $Hg[Co(NCS)_4]$ and doubly distilled water were used. The diamagnetic corrections were applied using the Pascal constants [21, 22]. The effective magnetic moments (μ_{eff}) per complex molecule were calculated using the formula $\mu_{eff} = \sqrt{8\chi_M T}$, where χ_M is the molar magnetic susceptibility including Pascal diamagnetic corrections.

RESULTS AND DISCUSSION

The objective of this study was the reaction of Fe^{3+} ions with 2*s* metal (Sr and Ba) salicylates in methanol–dimethylacetamide–tetrahydrofuran system to obtain heteronuclear salicylates. Compounds **I** and **II** in the crystals exist as coordination polymers in which the cations are connected into one-dimensional chains. In compound **I**, salicylic acid residues and the NO_3^- group perform bridging functions.

The independent part of the unit cell of **I** (Fig. 1) contains one trivalent iron atom and two divalent strontium atoms. Two doubly deprotonated (Sal^{2-}) and two singly deprotonated ($SalH^-$) salicylic acid residues and the NO_3^- anion serve as the counter-ions. Four DMA molecules are involved in the coordination as neutral ligands.

The iron(III) atom coordinates all independent salicylic acid residues. The iron coordination octahedron comprises two monodentate (with respect to iron) $SalH^-$ residues (Fe(1)–O(1), 2.015 Å; Fe(1)–O(4), 2.049 Å). Two Sal^{2-} residues are attached to Fe in the bidentate chelating mode through the oxygen atoms of the carboxyl and deprotonated hydroxyl groups (Fe–O, 1.952–1.979 Å).

The Sr(1) and Sr(2) atoms are surrounded by eight and seven oxygen atoms, respectively. The Sr(1) environment comprises two neutral DMA ligands (*A* and *B*) attached through the O(1*A*) and O(1*B*) atoms, the NO_3^- anion chelating the metal atom through O(13) and O(14), three carboxyl oxygen atoms of three salicylic acid residues ($O(2)^1$, $O(7)^1$, O(11)), and the phenol group atom ($O(12)^1$) (symmetry transformations are indicated in Table 2). The Sr(1)–O distances are in the range of 2.472–2.708 Å.

The seven-vertex polyhedron arranged around Sr(2) differs from that around Sr(1). The Sr(2) environment comprises two neutral DMA molecules coordinated through O(1*C*) and O(1*D*) atoms, the O(13) atom of the NO_3^- group, $O(5)^2$, O(8), and O(10) atoms of the carboxyl groups of the acid residues, and the $O(9)^2$ atom of

Table 2. Selected interatomic distances and bond angles in **I** and **II***

I

Fe(III) polyhedron

Bond	*d*, Å	Bond	*d*, Å
Fe(1)–O(1)	2.015(6)	Fe(1)–O(9)	1.973(6)
Fe(1)–O(4)	2.056(6)	Fe(1)–O(10)	1.977(6)
Fe(1)–O(7)	1.975(6)	Fe(1)–O(12)	1.953(6)
Angle	ω, deg	Angle	ω, deg
O(12)Fe(1)O(9)	177.7(3)	O(7)Fe(1)O(1)	92.8(3)
O(12)Fe(1)O(7)	89.6(2)	O(10)Fe(1)O(1)	89.4(2)
O(9)Fe(1)O(7)	91.1(2)	O(12)Fe(1)O(4)	89.6(2)
O(12)Fe(1)O(10)	90.9(2)	O(9)Fe(1)O(4)	88.3(3)
O(9)Fe(1)O(10)	88.2(2)	O(7)Fe(1)O(4)	86.5(2)
O(7)Fe(1)O(10)	177.7(3)	O(10)Fe(1)O(4)	91.3(2)
O(12)Fe(1)O(1)	91.9(2)	O(1)Fe(1)O(4)	178.4(3)
O(9)Fe(1)O(1)	90.3(2)		

Sr(1) and Sr(2) polyhedra

Bond	*d*, Å	Bond	*d*, Å
Sr(1)–O(1*A*)	2.472(7)	Sr(2)–O(8)	2.472(6)
Sr(1)–O(1*B*)	2.504(7)	Sr(2)–O(1*D*)	2.484(7)
Sr(1)–O(11)	2.548(6)	Sr(2)–O(1*C*)	2.517(6)
$Sr(1)–O(7)^1$	2.560(6)	$Sr(2)–O(5)^2$	2.566(6)
$Sr(1)–O(2)^1$	2.632(6)	$Sr(2)–O(10)^2$	2.591(6)
Sr(1)–O(14)	2.636(6)	$Sr(2)–O(13)^2$	2.631(6)
Sr(1)–O(13)	2.705(6)	$Sr(2)–O(9)^2$	2.664(6)
$Sr(1)–O(12)^1$	2.708(5)		

II

Fe(1) and Fe(2) polyhedra

Bond	*d*, Å	Bond	*d*, Å
Fe(1)–O(1)	2.0699(17)	Fe(2)–O(7)	2.0521(16)
Fe(1)–O(4)	1.9702(15)	Fe(2)–O(10)	1.9541(15)
Fe(1)–O(6)	1.9437(15)	Fe(2)–O(12)	1.9569(15)
Angle	ω, deg	Angle	ω, deg
O(4)Fe(1)O(6)	90.45(6)	O(7)Fe(2)O(10)	91.34(7)
O(1)Fe(1)O(6)	90.04(7)	O(7)Fe(2)O(12)	86.95(7)
O(1)Fe(1)O(4)	92.80(7)	O(10)Fe(2)O(12)	91.15(6)

Ba(1) and Ba(2) polyhedra

Bond	*d*, Å	Bond	*d*, Å
Ba(1)–O(2)	2.7540(18)	Ba(2)–O(8)	2.8206(17)
Ba(1)–O(4)	2.7548(16)	Ba(2)–O(10)	2.7978(15)
Ba(1)–O(11)	2.6867(17)	Ba(2)–O(14)	2.7865(18)
Ba(1)–O(16)	2.715(2)	Ba(2)–O(5)	2.6933(18)
Ba(1)–O(17)	2.659(2)	Ba(2)–O(18)	2.695(2)
Ba(1)–O(13)	2.7244(18)	Ba(2)–O(19)	2.7187(19)
Ba(1)–O(1w)	2.877(3)	$Ba(2)–O(12)^3$	2.9104(15)
Ba(2)–O(13)	2.9549(18)		

* Symmetry transformations for equivalent atoms of **I**: [1] *x* + 1, *y*, *z*; [2] *x* – 1, *y*, *z*; **II**: [3] –*x*, –*y*, –*z*.

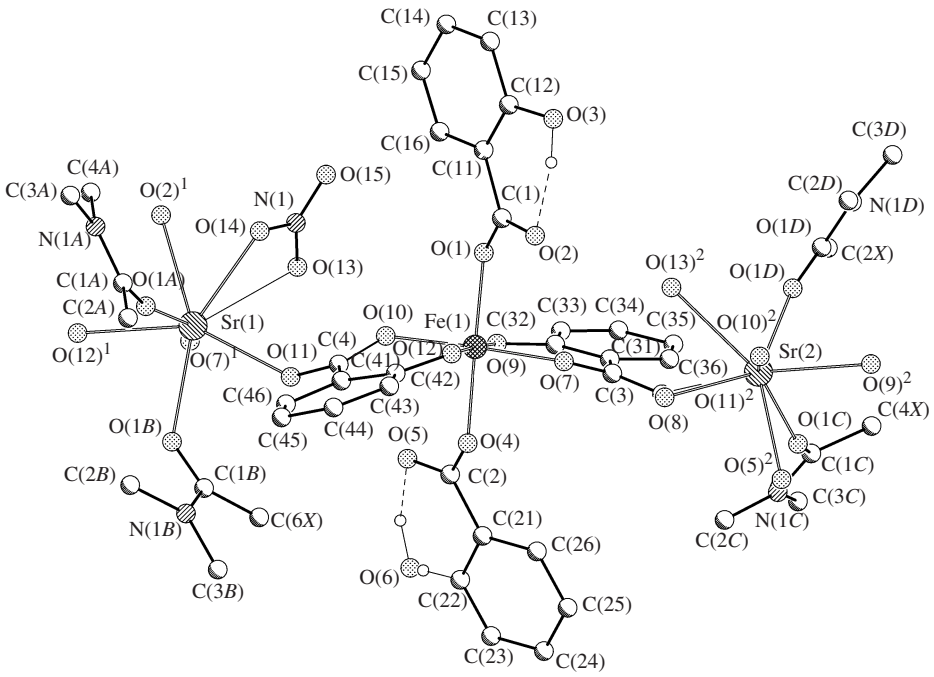

Fig. 1. Structure of the molecule of complex $\{[FeSr_2(Sal)_2(SalH)_3(DMA)_4(H_2O)]\}_n$ (**I**).

the hydroxyl group. The Sr(2)–O distances are 2.472–2.667 Å.

The NO_3^- group in **I** is coordinated in the tridentate chelating bridging mode.

The two monodeprotonated $SalH^-$ residues are bidentate and form *syn-syn* bridges between iron and strontium atoms (Fe(1)–Sr(1), 3.602; Fe(1)–Sr(2), 3.636 Å). Two doubly deprotonated Sal^{2-} residues are pentadentate. Apart from the *syn-syn* bridging oxygens, one oxygen of the Sal^{2-} carboxyl performs a μ_2-O function between Fe and Sr atoms. The same function is performed by the deprotonated hydroxyl group. The diverse coordination modes of the carboxyl groups are described systematically in the review by M. A. Porai-Koshits [23]; the structural functions of the carboxyl groups of salicylic acid found in **I** fit into his scheme. The ability of the carboxyl group to form bridging systems makes it promising for the synthesis of clusters and coordination polymers. In compound **I**, the polymer axis is directed along the *x* axis of the crystal. The coordinated hydroxyl groups of salicylic acid form a system of hydrogen bonds (Table 3). In the crystal, the polymeric chains are located at the van der Waals distances of the radii.

The structure of compound **II** (Fig. 2) is similar to **I** with the difference that **II** contains a coordinated water molecule and the role of the NO_3^- group is played by an additional singly charged salicylic acid residue $SalH^-$. In this case, the ratio Fe : Ba : acid residue = 1 : 2 : 5 (unlike the ratio Fe : Sr : acid residue : NO_3^- = 1 : 2 : 4 : 1 in **I**).

However, the arrangement of the coordination polymer **II** has some special features. First of all, Fe(1) and Fe(2) atoms occupy two special positions at the inversion centers. The slightly distorted octahedron of each of Fe(1) and Fe(2) atoms is formed by four carboxylate and two hydroxyl oxygen atoms of salicylic acid. One acid residue is attached to iron in the bidentate chelating mode to give a six-membered metal ring (Fig. 2). In the metal rings, the average Fe–O distances are 1.956 Å (equatorial) and 2.060 Å (apical). The same tetragonal distortion effects of the metal coordination polyhedron were also found in **I**.

The Ba(1) coordination polyhedron is formed by eight oxygen atoms. These include the oxygen atoms of three DMA ligands disordered with equal probability over two positions, four O atoms of the carboxylate and hydroxyl groups of the $SalH^-$ and Sal^{2-} residues, and the O atom of the water molecule. The coordination number equal to 8 is also typical of Ba(2) atom with the difference that the $O(H_2O)$ position is occupied by oxygen of the $SalH_2$ carboxyl group.

As noted above, the crystal of **II** contains five salicylic acid residues: two doubly deprotonated (Sal^{2-}) and three deprotonated at the carboxyl group ($SalH^-$). In the latter ligands containing C(11)–C(16), C(31)–C(36), and C(51)–C(56) atoms of the benzene rings, two deprotonated carboxyl groups at the C(1) and C(3) atoms function as a bidentate *syn-syn* bridge by linking

Table 3. Characteristics of hydrogen bonds in structures **I** and **II**

D–H···A	Distance, Å			DHA angle, deg	Transformation for A atom
	D–H	H···A	D···A		
$\{[FeSr_2(Sal)_2(SalH)_2(NO_3)(DMA)_4]\}_n$ (**I**)					
O(3)–H···O(2)	0.93	1.76	2.614(9)	152	
O(6)–H···O(5)	0.91	1.85	2.57(1)	135	
$\{[FeBa_2(Sal)_2(SalH)_3(DMA)_4(H_2O)]\}_n$ (**II**)					
O(1*w*)···H	0.92	1.88	2.749(4)	158	
O(1*w*)···H	0.91	1.92	2.789(5)	159	$1 - x, -y, -z$
O(9)···H	0.89	1.86	2.553(3)	133	
O(15)···H	0.94	1.72	2.556(3)	146	
O(3)···H	0.87	1.72	2.497(4)	147	

the barium and iron atoms. The tridentate chelating bridging carboxylate group at C(5) connects two Ba atoms.

Two doubly deprotonated Sal^{2-}ligands are pentadentate and are the key structuring unit of the coordination polymer in the crystal. The polymeric chains along the *x* axis of the crystal are combined by hydrogen bonds (Table 3).

Compounds **I** and **II** have intricate IR spectra with numerous absorption bands (see Experimental). The IR absorption regions above 2500 cm^{-1} are different for complexes **I** and **II** (3300–3550 cm^{-1}) with a peak at 3434 cm^{-1}, which can be attributed to ν(OH) stretching modes of coordinated water molecules involved in intra- and intermolecular hydrogen bonds.

The DMA methyl groups are responsible for asymmetric and symmetric ν(CH) stretching vibrations (2990, 2940, 2880, and 2864 cm^{-1}), asymmetric and symmetric δ(CH) bending vibrations (1380–1200 cm^{-1}), and ρ(CH) rocking vibrations (1200–800 cm^{-1}). The presence of salicylic acid anions in **I** and **II** is manifested as bands at 3070, 3040, 1600, 1580, and 1518 cm^{-1} assigned to the ν(CH) (aromatic ring) and ν(CC) + δ(CCH) vibrations. The carboxyl groups of salicylic acid anions coordinated in different fashions account for asymmetric and symmetric ν(COO) stretching bands at 1620, 1600, 1470, 1472, and 1423 cm^{-1}. The corresponding absorption bands (ν(C–O), δ(OH), δ(COO), and so on) in the low-frequency spectral region also attest to several modes of coordination of $SalH^-$ and Sal^{2-} residues to metal atoms.

According to X–ray diffraction data for **I** and **II**, the DMA molecules are coordinated to metal atoms through carbonyl oxygen atoms. As a result of coordination, the ν(C=O) stretching band of free DMA (1570 cm^{-1}) shifts to lower frequencies in **I** and **II** by Δν(C=O) of ~50 cm^{-1}, which is consistent with reported data [24, 25]. In the IR spectra of outer-sphere DMA molecules forming C=O···H hydrogen bonds, the ν(C=O) mode is shifted to lower energy by only 10–15 cm^{-1} [24, 25].

The presence of the nitrate group and its coordination to the metal atom in **I** is manifested in the IR spectrum by bands at 1423 $\nu_{as}(NO_2)$, 1305 $\nu_s(NO_2)$, and 1015 (ν(NO) cm^{-1} [26]. The IR spectra of **I** and **II** contain absorption bands at 623–440 cm^{-1}, which can be assigned to ν(FeO), ν(SrO), and ν(BaO) stretching vibrations [26].

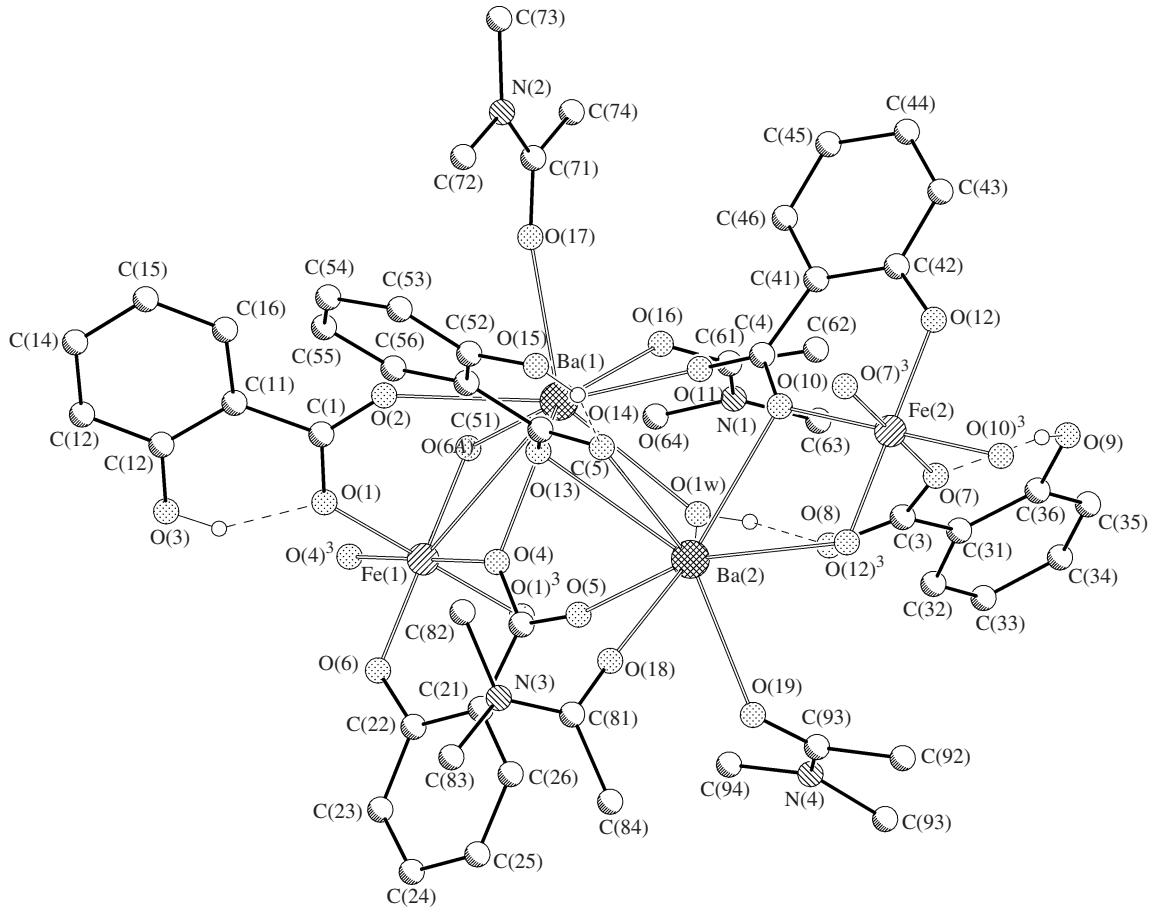

Fig. 2. Structure of the molecule of complex $\{[FeBa_2(Sal)_2(SalH)_3(DMA)_4(H_2O)]\}_n$ (**II**).

CTA data (Table 4) show that decomposition of strontium complex **I** is stepwise. The first two effects are endotherms related to successive removal of DMA molecule and two singly charged $SalH^-$ anions.

The next four processes (260–460°C) are exothermic and end in the formation of strontium carbonate and iron(III) oxide. The range of 580–850°C shows two endotherms apparently related to decomposition of strontium carbonate. The final decomposition product is mixed oxide, $0.5\,Fe_2O_3 \cdot 2SrO$, corresponding to 24% of the weight of initial complex **I**, which is consistent with the calculated value (24.2%).

Thermal decomposition of complex **II** is also stepwise. The first effect (50–120°C) is accompanied by weight loss of ~7%, which corresponds to removal of one water molecule and one DMA molecule (the calculated value is 7.6%). Note that decomposition of barium complex **II** starts at 50°C, which is 40°C lower than that for strontium compound **I**. At temperatures above 120°C, the DTG curve clearly shows two regions, 124–265°C and 265–400°C, each comprising two overlapping processes with peaks at ~190 and ~220°C, ~310 and ~390°C. The thermal decomposition phase (124–265°C) is accompanied by a total weight loss of 36% and is apparently related to the removal of all monodentate molecules (four DMA and H_2O) and partial decomposition of the salicylate ligands. Above 420°C, the DTG and DTA curves of **II** do not record any processes, although the TG curve shows monotonic decrease in the weight by 3–4% in the range of 420–800°C. The mixed oxide $2BaO \cdot 1/2Fe_2O_3$ (29–26%, theoretically 28%) is formed from **II** as the final thermal decomposition product.

The effective magnetic moment per iron atom in **I** at room temperature (5.88 μ_B) corresponds to high-spin ($S = 5/2$) Fe(III) ions, which is consistent with published data [21, 22] for FeO_6 local environment of Fe^{3+} ion forming a weak ligand field.

The structural investigation of heterometallic coordination polymers reveals self-organization of components of the reaction medium needed for meeting the conditions for linking of metal atoms in the structure by bridges. It was shown that the structural functions of salicylic acid residues are different, their denticity ranging from 1 to 5. Their bridging functions are also diverse, which shows itself in the IR spectra. The Fe^{3+}

Table 4. Thermogravimetric data for complex **I***

Effect	*T*, °C		Weight loss. %,
	onset	end	found
endo	90	190	20.0
endo	190	260	15.0
exo	260	340	14.5
exo	340	370	5.0
exo	370	420	10.0
exo	420	460	4.5
endo	580	650	3.5
endo	740	850	3.5

* The weight of the final product was 24% of the initial weight.

coordination unit FeO_6 characterizes a weak ligand field.

REFERENCES

1. Cannon, R.D. and White, R.P., *Prog. Inorg. Chem.*, 1988, vol. 36, p. 195.
2. Sheriff, S., Hendrickson, W.A., and Smith, J.L., *J. Mol. Biol.*, 1987, vol. 197, no. 2, p. 273.
3. Rosenzwieg, A., Norlund, C.A., Frederick, C.A., and Lippard, S.J., *Nature (London)*, 1993, vol. 366, p. 537.
4. Harrison, P.M., Hempstead, P.D., Artymiuk, P.J., and Andrews, S.C., *Metal Ions in Biological Systems*, New York: Marcel Dekker Inc., 1998, vol. 35, ch. 11, p. 435.
5. Long, J.R., *Molecular Cluster Magnets: Chemistry of Nanostructured Material*, Yang. P., Ed., Hong Kong: World Scientific, 2003.
6. Diakite, K., Zhan, D., and Zhang, K., *Mater. Lett.*, 2005, vol. 59, no. 19, p. 2243.
7. Jha, F.R. and Mishra, H.C., *Chim. Acta Turc.,* 1986, vol. 14, no. 1, p. 51.
8. Aggett, J., Crossley, P., and Hancock, R., *J. Inorg. Nucl. Chem.*, 1969, vol. 31, no. 1, p. 3241.
9. Tel'zhenskaya, P.N. and Shvarts, E.M., *Koord. Khim.*, 1977, vol. 3, no. 9, p. 1279.
10. Boons, C.H.M., Spala, E., and van Dam, W., EP Patent 1489159, 2004-12-22.
11. Amalraj, A.J., Sundaravadivelu, M.A., Regis, P.P., and Rajendran, S., *Anti-Corros. Methods Mater.*, 2001, vol. 48, no. 6, p. 371.
12. Tkahashi, M., Kurosawa, O., Ando, J., et al., EP Patent 1816183, 2007-08-08.
13. Roth, G.J. and Calverley, D.C., *Blood*, 1994, vol. 83, no. 4, p. 85.
14. Olednik, V., Turte, K., Shova, S., et al., Abstracts of Papers, *XXII mezhdunar. Chugaev. konf. po koordinatsionnoi khimii* (XXII Intern. Chugaev. Conf. on Coordination Chemistry), 2005, p. 450.
15. Olednic, V., Shova, S., Prodius, D., et al., Abstracts of Papers, *The XV Int. Conf. "Physical Methods in Coordination and Supramolecular Chemistry" and the XVII Reading in Memory of Acad. A. Ablov*, 2006, p. 72.
16. Olednic, V., Shova, S., Mereacre, V., et al., Abstracts of Papers, *A XXIX-a Conferintá Nationalá de Chimie*, Calimanesti-Caciulata, 2006.
17. Olednik, V.V., Turte, K.I., Simonov, Yu.A., et al., Abstracts of Papers, *XXIII mezhdunar. Chugaev. konf. po koordinatsionnoi khimii* (XXIII Intern. Chugaev. Conf. on Coordination Chemistry), 2007, p. 558.
18. Otwinowski, Z. and Minor, W., *Methods Enzymol.,*1997, vol. 276, p. 307.
19. *XEMP. Version 4.2,* Siemens Analytical X-ray Inst. Inc., 1990.
20. Sheldrick, G.M., *SHELX-97 Manual,* Göttingen (Germany): Univ. of Göttingen, 1997.
21. Kalinnikov, V.T. and Rakitin, B.V., *Vvedenie v magnetokhimiyu. Metod staticheskoi magnitnoi vospriimchivosti v khimii* (Introduction to Magnetocemistry. The Method of Static Magnetic Susceptibility in Chemistry), Moscow: Mir, 1980.
22. Kahn, O., *Molecular Magnetism*, New York: VCH, 1993.
23. Porai-Koshits, M.A., *Itogi Nauki Tekh., Ser. Kristalokhim.*, Moscow: VINITI, 1981 vol. 15.
24. Tsintsadze, M.T., Kharitonov, Yu.Ya, Tsivadze, A.Yu., et al., *Koord. Khim.*, 1996, vol. 22, nos. 7–8, p. 524.
25. Fujcate, M., Kubota, Y., and Ohasi, N., *J. Mol. Spectrosc.*, 2006, vol. 236, no. 1, p. 97.
26. Nakomoto, K., *Infrared and Raman Spectra of Inorganic and Coordination Compounds*, New York: Wiley, 1986.